Structural and vibrational analysis of amorphous Au_{55} clusters

Ignacio L. Garzón
Instituto de Física, Universidad Nacional Autónoma de México, Apartado Postal 2681, Ensenada, Baja California 22800, Mexico

Alvaro Posada-Amarillas
Programa de Posgrado en Física de Materiales, Centro de Investigación Científica y de Educación Superior de Ensenada, Apartado Postal 2681, Ensenada, Baja California 22800, Mexico
and Centro de Investigación en Física, Universidad de Sonora, Apartado Postal 5-088, Hermosillo, Sonora 83000, Mexico
(Received 17 June 1996)

We present a structural and vibrational analysis of several amorphous (disordered) and ordered isomers of a 55-atom gold cluster. A Gupta *n*-body potential, with parameters fitted to gold clusters, was used to model the metallic bonding in the Au_{55} cluster. The molecular-dynamics method combined with simulated annealing and quenching techniques were used to perform the cluster structure optimization. Our results show that several nonequivalent and nearly degenerate in energy amorphous cluster structures are more stable than those with high symmetry like the 55-atom Mackay icosahedron and the fcc cuboctahedron. The calculated distribution of normal frequencies clearly discriminates between amorphous and ordered cluster configurations and confirms their stability. A common-neighbor analysis was implemented to characterize the disordered cluster structures, identifying the short-range order of the amorphous phase, according to the local environment of each atom pair in the cluster. Distorted multilayer icosahedral order was found to be the more representative of the amorphous clusters with the lowest energies. At higher energies, the amorphous structures are characterized by the presence of distorted local icosahedral order. The origin of the higher stability of amorphous vs ordered isomers in Au_{55} is in the short range of the *n*-body interaction existing in the metal cluster bonding. [S0163-1829(96)06540-X]

I. INTRODUCTION

The study and characterization of structural and dynamical properties of clusters in amorphous phase is becoming an interesting field of research in cluster science.[1] However, few of these systems have been investigated at present, both theoretically or experimentally. The computer simulation study of glassy $(KCl)_{32}$ (Ref. 1) and the high resolution transmission electron microscopy (HRTEM) experiments on amorphous Au and Pd nanoparticles[2] are recent developments in this direction.

The concept of glassy or amorphous clusters was introduced by Rose and Berry (RB) (Ref. 1) using computer simulation studies on structural properties of the alkali halide cluster $(KCl)_{32}$. It was shown that this cluster is large enough to present well defined ordered and disordered stable structures. RB defined the microamorphous state of a cluster and how to characterize it, according to a classification of inherent structures[3,4] associated to basins of the cluster multidimensional potential energy surface (PES). Born-Mayer and shielded Coulomb pair potentials were used for testing different forms of producing amorphous ionic clusters. The range of the potential was found to be important in reducing the cooling rate during the cluster amorphization.[1]

Theoretical evidence on the existence of disordered structures as low-energy configurations of metal clusters has also been reported.[5,6] In an *ab initio* study of the Car-Parrinello type on Al clusters,[5] it was shown that Al_{55} presents substantial structural distortions in its lowest-energy configuration with respect to the highly symmetric icosahedral and cuboctahedral structures. Several inequivalent and nearly degenerate disordered structures were found for the 55-atom aluminum cluster. The large distortions in the structures of several isomers of Al_{55} were associated to the short range of the screened interatomic interactions. Similar results were reported for the Pt_{55} cluster in a simulated annealing Monte Carlo study, using an embedded atom method (EAM) potential.[6]

It is interesting to notice that amorphous clusters are not only found as computer simulated samples. Recently, HRTEM studies on gold and palladium nanoparticles reported images of polycrystalline and amorphous structures in the particle size range of a few nanometers.[2] In other HRTEM experiments, the transition between crystalline and amorphous structures in gold nanoclusters was recorded.[7] However, the specific conditions for the growth of amorphous metal small particles have not yet been determined.

Motivated by the interest generated by the above research, we investigate the existence of a microamorphous state[1] in gold clusters. Several theoretical[8–11] and experimental[7,12,13] studies on the structure and stability of Au_n clusters have been reported in the literature. Theoretical calculations based on the *n*-body Gupta potential suggest that the most stable structure of the Au_{55} cluster is icosahedral.[9–11] On the other hand, the experimental information is still uncertain assigning cuboctahedral[12] and icosahedral[13] structures to such a cluster. Nevertheless, although the theoretical studies[9–11] agree about the higher stability of the icosahedral configuration with respect to the fcc cuboctahedron, none of them have explored the existence of other stable isomers with different symmetry, through a fully dynamical optimization procedure.

 © 1996 The American Physical Society

In this work, we show that the Au_{55} cluster can be found in amorphous (disordered) stable structures and, even more importantly, these disordered structures are more stable than configurations with high symmetry like the 55-atom Mackay icosahedron and the fcc cuboctahedron. Our methodology is similar to that used by RB (Ref. 1) to study ionic amorphous clusters. The multidimensional PES of the Au_{55} cluster is generated with a Gupta n-body potential. The molecular-dynamics method and simulated annealing and quenching techniques are used to obtain minima of the PES associated to stable cluster isomers. A structural and vibrational analysis of several amorphous and ordered isomers of the Au_{55} cluster is performed to discriminate between both types of structures and check their stability. A common-neighbor analysis[14,15] is implemented to have a quantitative characterization of the disordered cluster structures. With this method, the kind of short-range order existing in the amorphous clusters is extracted, according to the local environment of each atom pair in the system.

The details of the potential energy and simulation method are described in Sec. II. The structural and vibrational properties of the Au_{55} cluster isomers and a discussion of them are presented in Sect. III. In Sec. IV, we use the common-neighbor analysis to classify and give a quantitative description of the cluster disordered structures. Section V contains the summary and conclusions of this work.

II. GUPTA POTENTIAL AND SIMULATION METHOD

The metallic bonding in Au_n clusters is modeled through an n-body potential coming from Gupta's expression[16] for the cohesive energy of transition and noble metals. The attractive term of the interatomic interaction is derived within a second-moment approximation of a tight-binding model in which n-body effects are included.[17] The repulsive part is a sum of pairwise Born-Mayer terms. As a function of the interatomic distance r_{ij}, it is written as

$$V=\frac{U_n}{2}\sum_{j=1}^{n}\left[A\sum_{i(\neq j)=1}^{n}\exp[-p(r_{ij}/r_{0n}-1)]-\left(\sum_{i(\neq j)=1}^{n}\exp[-2q(r_{ij}/r_{0n}-1)]\right)^{1/2}\right], \qquad (1)$$

where the parameters p, q, and A depend on the material. The remaining two parameters U_n and r_{0n} are not only material dependent but also size dependent, which is indicated by attaching the subscript n to them ($n=55$, in the present case). In this work we adopt the values $p=10.15$ and $q=4.13$, which have been fitted for bulk gold.[18] The value $A=0.118\,438$ is obtained when the cohesive energy of the fcc metal at the equilibrium value of its nearest-neighbor distance converges. The parameters U_{55} and r_{055} can be fitted to experimental or *ab initio* data of the 55-atom gold cluster binding energy and nearest-neighbor distance. Using extended x-ray-absorption fine-structure spectroscopy (EXAFS) results[13] for the nearest-neighbor distance and assuming Equation 4 of Ref. 8, with EAM results for the binding energy of the 55-atom nickel cluster,[19] we estimate and use the values $r_{055}=2.96$ Å and $U_{55}=3.454$ eV.

The Gupta potential given in Eq. (1) has been used to study structural and thermodynamical properties of fcc (Refs. 18 and 20) and hcp transition metals and alloys.[20] Structural, dynamical, meltinglike,[8,21–23] fragmentation,[24] and vibrational[25,26] properties of metal clusters have been extensively studied using the Gupta n-body potential in molecular-dynamics simulations. In this work, we extend its range of applications to describe structural and vibrational properties of amorphous Au_{55} clusters.

Computer simulated amorphous samples were obtained combining the constant energy molecular-dynamics method and simulated annealing and quenching techniques.[8,21–23] The Newton's equations of motion were solved using the velocity Verlet algorithm[27] with a time step of 2.3×10^{-15} s. This time step assures conservation of total energy, even in the longest run (10^5 time steps), within 0.5%. Simulated annealing and quenching techniques are the best currently available procedures to find global and local minima in complicated (large n) situations. They allow us to test the results varying cooling rates and starting configurations. The structures obtained using such methods correspond to stable configurations associated to minima of the cluster multidimensional PES. In a typical calculation, we used a liquidlike cluster structure[28] at about $T=1100$ K as initial configuration and performed MD simulations in which the total energy was decreased until the cluster structure no longer changed on further cooling ($T=10^{-4}$ K). Several initial conditions taken from trajectories of the liquidlike cluster and cooling rates in the range of $10^{11}-10^{13}\,\mathrm{K\,s^{-1}}$ were used to obtain stable Au_{55} cluster isomers as minima of the PES. The structural and vibrational properties of these clusters are described in the next section.

III. STRUCTURAL AND VIBRATIONAL ANALYSIS

A set of nonequivalent nearly degenerate cluster structures was obtained following the optimization procedure discussed above. All of them correspond to disordered configurations of the Au_{55} cluster. Three of the lowest-lying isomers and their energies are shown in the upper panels on the left of Fig. 1. The 55-atom Mackay icosahedron and fcc cuboctahedron are also shown on the lower left panels of the same figure, together with their energies, which were obtained relaxing such structures using a simulated quenching procedure.[8,21,23] Notice that the disordered isomers are more stable than the high symmetry icosahedron and cuboctahedron clusters. The higher stability of disordered metal cluster isomers with respect to symmetric ordered structures was also found in Al_{55} using the *ab initio* Car-Parrinello method[5] and in Pt_{55} with an EAM potential.[6] This behavior contrasts with the one observed in the $(KCl)_{32}$ ionic cluster where the rock-salt crystalline structure is more stable than the amorphous isomers.[1] Rare-gas atom clusters modeled with a Lennard-Jones potential also have a highly symmetric icosahedral structure as the lowest-energy configuration for $n=55$ and other magic numbers.[29]

Since the optimization procedure does not guarantee that the lowest-energy Au_{55} amorphous cluster (AMO0) corresponds to the global minimum of the PES, it could be possible that ordered or highly symmetric structures other than the icosahedron or cuboctahedron exist with lower energy

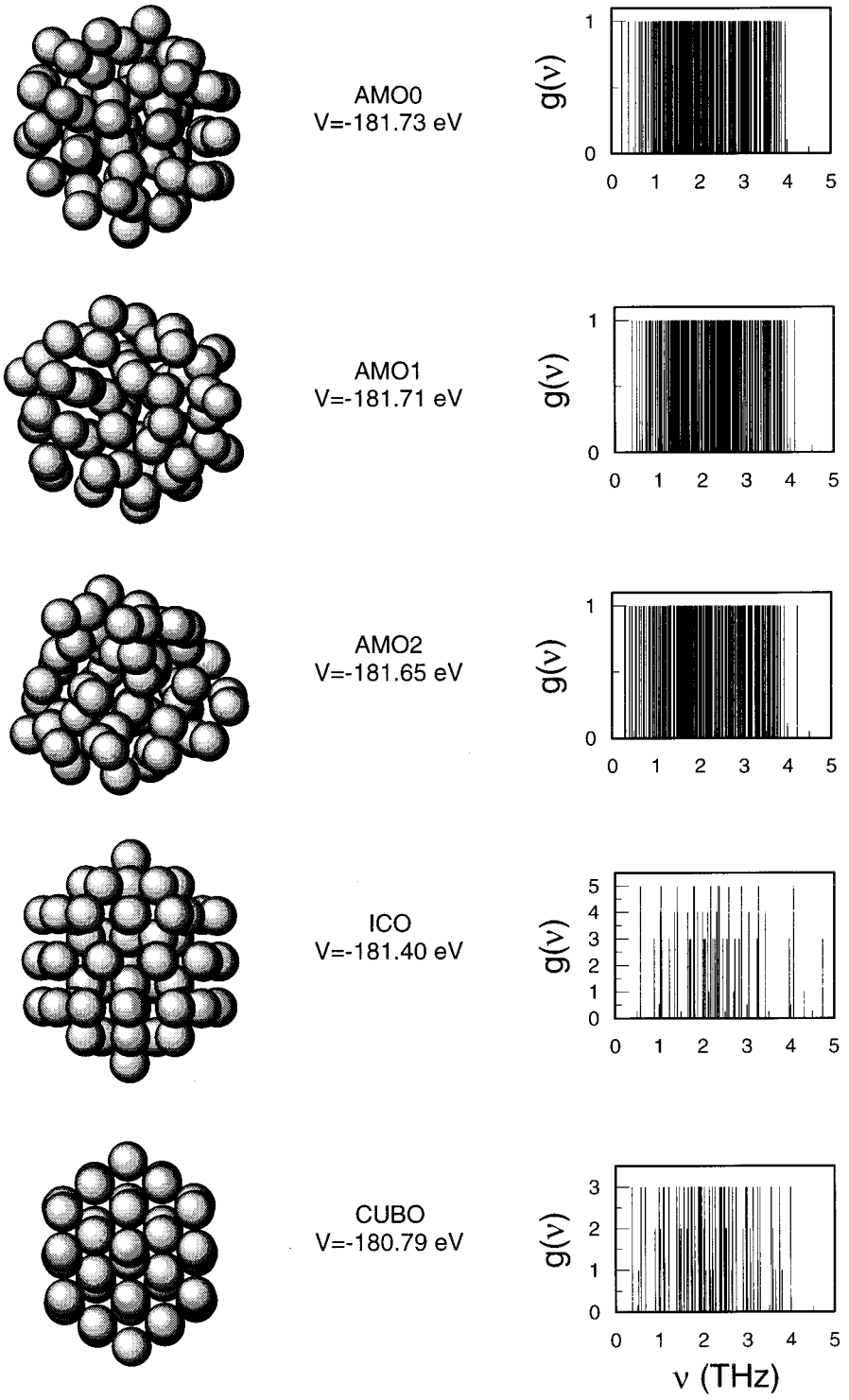

FIG. 1. Left: stable isomers and their energies (in eV) of the Au_{55} cluster. The three upper configurations correspond to amorphous gold clusters. The cluster shown on the top was the lowest-energy configuration obtained in several optimization procedures performed. The icosahedron and cuboctahedron structures and their energies are also given for comparison. Right: Vibrational spectra of the five isomers. The vertical axis shows the degree of degeneracy.

values. However, none of these ordered configurations were seen in any of the various annealing procedures performed, even at the slowest cooling rate ($10^{11}\,K\,s^{-1}$) computationally available. In the quenching simulations of the KCl_{32} cluster[1] an opposite behavior was found. The amorphous structures were only obtained using cooling rates higher than $10^{13}\,K\,s^{-1}$, otherwise crystallike structures (regular and defected) were found. To reach amorphization with a cooling rate of the order of $10^{11}\,K\,s^{-1}$ the range of the pair potential needed to be reduced using a shielded Coulomb interaction.[1]

Therefore, our results suggest that the topology of the PES of the Au_{55} cluster is characterized by low-energy minima corresponding to disordered cluster configurations whereas symmetric ordered structures would have higher energies. Then, the picture emerging for the topology of this PES is qualitatively different from that described by RB for the amorphous $(KCl)_{32}$.[1] In that case, the amorphous minima are at higher energies than those corresponding to a crystalline structure.

The above differences can be explained in terms of the short range of the n-body interaction potential. Several structures for the 55-atom cluster are possible because most of the atoms are on the surface and are almost free from the constraints of bulk packing. Small changes in the positions of distant neighbors can lead to different structures. In the present case, the range of the n-body interaction is governed by the parameters p and q of the Gupta potential. These parameters were fitted to bulk properties of gold.[18] In other studies,[21,22] we have done similar calculations for nickel clusters using a different set of parameters. In that case, the range of the interaction was longer ($p=9$, $q=3$) and consequently the low-lying isomers of Ni_{55} correspond to ordered highly symmetric structures.[22] A similar behavior was found between Pd_{55} and Pt_{55} clusters studied with EAM potentials.[6] Their lowest-energy configurations are the icosahedron and a disordered configuration, respectively. It is expected that the range of the n-body interaction in Pd clusters will be longer than in Pt clusters. The values of the parameters p and q of the Gupta potential for Pd and Pt fitted to bulk properties,[18,20] are consistent with this interpretation. A systematic study of the effect of the range of two-body interactions on the structures of clusters was reported recently, using a Morse potential.[30]

The cluster atomic configurations can be used to evaluate the second derivatives of the potential energy with respect to the atomic coordinates. These values generate the elements of the dynamical matrix. A numerical diagonalization of this matrix was performed to obtain the normal frequencies and eigenvectors.[26] Six of the calculated $3n$ eigenvalues are equal to zero, corresponding to translational and rotational motions. The remaining $3n-6$ frequencies are the vibrational normal modes. The panels on the right of Fig. 1 show the normal frequencies distribution of the amorphous, icosahedron, and cuboctahedron Au_{55} isomers. The vertical axis counts the degeneracy of the modes. As expected, the amorphous structures have nondegenerate frequency spectra due to the absence of spatial symmetry. In contrast, the highly symmetric icosahedral structure shows normal modes with fivefold, fourfold, and threefold degeneracy plus a few nondegenerate modes associated to radial motions. The cuboctahedral structure has normal modes with threefold and twofold degeneracy and also single breathing modes. Except for the absence of sixfold and fivefold degenerate modes in the cuboctahedral structure, our results for the vibrational modes of the ordered isomers agree with those calculated using a similar potential.[10]

There are other interesting features in the vibrational properties of the Au_{55} clusters. The vibrational spectra of the amorphous isomers are shifted to lower frequencies with respect to the icosahedron normal modes distribution. This makes the amorphous clusters less stiff than the icosahedral isomer. Aside from the clear difference between ordered and disordered cluster configurations given through their frequency spectra, some differences are also displayed between the vibrational modes distribution of amorphous clusters. In particular, it is notorious that in the lowest-energy isomer (AMO0) with a configuration not far from the icosahedron, there exists a high density of modes toward the middle of the distribution, whereas in the more disordered third lowest-lying isomer (AMO2) the frequency distribution is more homogeneous along the whole range of frequencies.

Figure 2 shows the distribution of bond lengths (left) and the cluster pair distribution function (PDF) (right) for the five cluster configurations under consideration. The structural differences between amorphous and ordered Au_{55} isomers are well illustrated by both quantities. A clear tendency toward more uniform distributions is characteristic of the amorphous phase. The splitting of the second peak in the PDF, characteristic of bulk amorphous metals,[15] is already present in the 55-atom amorphous metal clusters. This feature is an additional signature of the degree of amorphization in this metal cluster. The peculiarities of the distributions of bond lengths and PDF's shown in the three upper panels of Fig 2 and their resemblance to those corresponding to bulk amorphous metals[15] confirm and justify the use of the term *amorphous* to describe the disorder in the atomic configurations under consideration. To better quantify the amount of disorder in the amorphous cluster samples, a classification of the short-range order can be done through a decomposition of the first and second peaks of the PDF's. The next section is dedicated to such analysis.

IV. COMMON-NEIGHBOR ANALYSIS

The degree of disorder in a noncrystalline material (bulk or cluster) can be quantified using the common-neighbor analysis (CNA) method.[14] Recently, such an approach has been used to investigate the microstructure of bulk liquid and amorphous Ni.[15] This method was also useful to study structural properties of Lennard-Jones clusters.[29] It is able to decompose the first and second peaks of the PDF by characterizing the local environment surrounding each atomic pair that contributes to the peaks of the PDF, in terms of the number and properties of common nearest neighbors of the pair under consideration. Additional details and advantages of the CNA method can be found elsewhere.[14,15] Here, we applied such a scheme to the five Au_{55} isomers shown in Fig. 1.

Table I shows the normalized abundance of selected pairs for the five isomers of the Au_{55} cluster. These quantities are normalized such that the total number of pairs contributing to the first peak of the PDF is unity. The classification of atom pairs in the cluster according to their common neighbors distinguishes between the two ordered structures: icosahedron and cuboctahedron (fifth and sixth columns of Table I, respectively). The main difference is that pairs type 1211 and 1421, characteristic of fcc clusters, are absent in the icosahedral configuration. In contrast, pairs type 1321, 1422, and 1551, typical of icosahedral structures, do not exist in the fcc cuboctahedron. Other types of pairs (1311, 2101, 2211, 2331, and 2441) are present in both structures but their relative abundance is different.

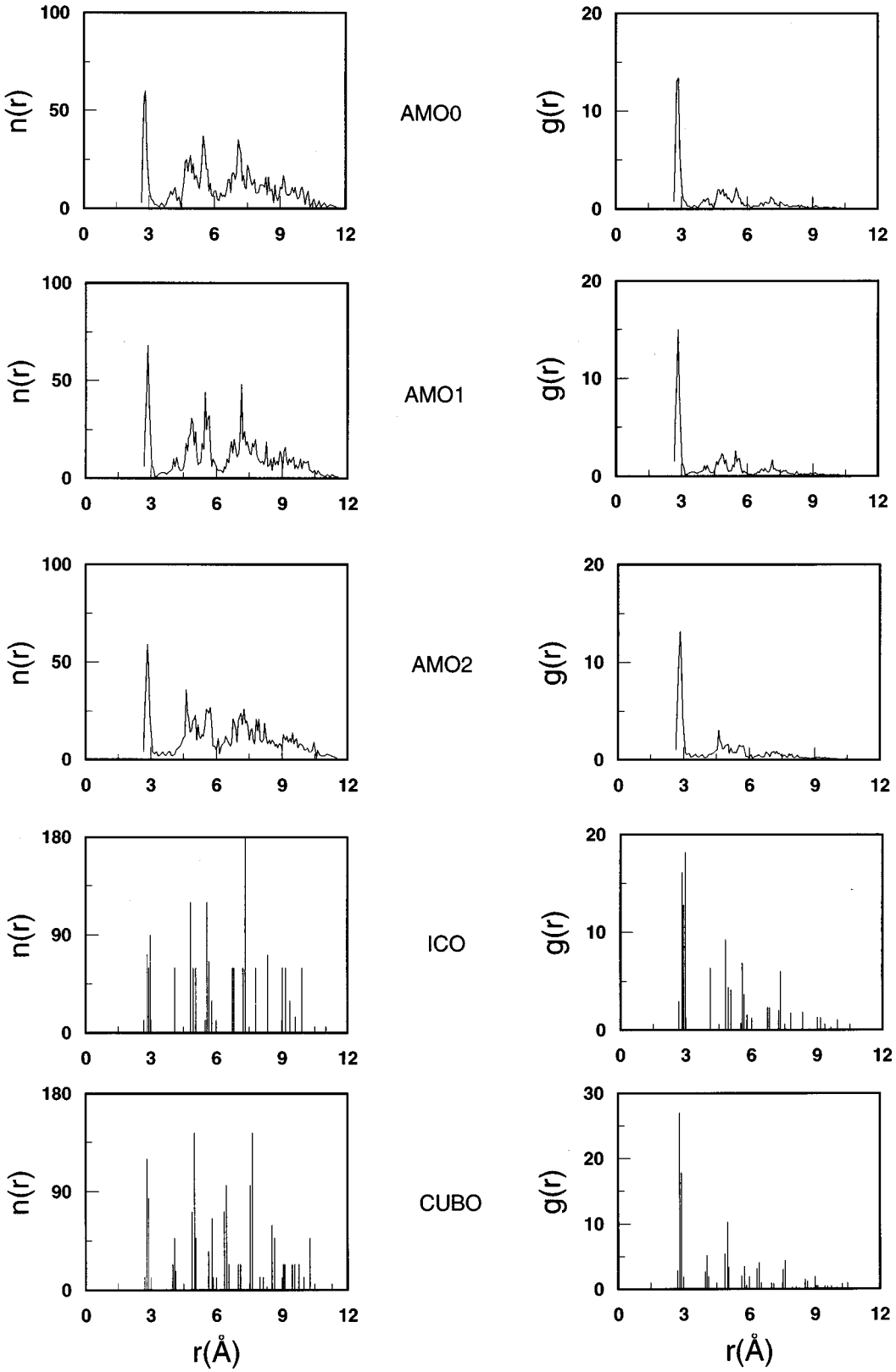

FIG. 2. Distribution of interatomic distances (left) and pair distribution function (right) of the five Au_{55} isomers shown in Fig.1.

A CNA analysis was done on Lennard-Jones clusters of several sizes[29] to define the local icosahedral order, characteristic of a 13-atom icosahedron, as that in which pairs type 1551 and 2331 are present in the absent of 1421, 1422, and 2441 pairs. Multilayer icosahedral order, characteristic of a 55-atom icosahedron, was also defined through the presence of pairs type 1422, 2441, and probably 1421 and a small but nonzero number of 2331 and 1551 pairs. Crystalline order was characterized by the presence of pairs type 1421, 1422, and 2441.[29]

A larger number of types of pairs appears in the amorphous Au_{55} clusters indicating the existence of more complex structures. The more abundant in the two lowest-lying isomers (second and third columns of Table I) are the pairs type 1311, 1321, 1422, 2101, 2211, and 2331, which are also the more abundant in the 55-atom icosahedron structure. In addition, a small number of other types of pairs is also present. This reveals that the structure of the two lowest-lying isomers is formed by a small distortion of the multilayer 55-atom icosahedron. Therefore, we can say that the lowest-energy configuration of the Au_{55} cluster is amorphous and its local environment is characterized by the presence of distorted multilayer icosahedral order. At higher energies, but still below the energies of the ordered structures, we found stable amorphous structures with distorted local icosahedral order, characterized by an increase in the abundance of pairs type 1551, 1541, and 2331. The third lowest-lying disordered isomer (fourth column of Table I) is a typical example of this class of amorphous clusters. The above results show that the short-range order in amorphous Au_{55} clusters is qualitatively different from the one observed in bulk amorphous transition metals (Ni),[15] where crystalline and local icosahedral (regular and distorted) atomic configurations were observed. However, for a better comparison, a study of the local order in bulk amorphous gold is necessary.

TABLE I. Normalized abundance of selected pairs for the five isomers of the Au_{55} cluster shown in Fig. 1. The atom pairs are characterized by four indices. The first index denotes the peak of the PDF to which the pair belongs. The second index counts the number of common nearest neighbors of that pair. The third index specifies the number of nearest-neighbor bonds found between the number of particles denoted by the second index. A fourth index is necessary to distinguish configurations with the same first three indices but being topologically different. The position of the first and second minima of the PDF is used as a cutoff distance to define the nearest-neighbor and second nearest-neighbor particles, respectively.

Pair	AMO0	AMO1	AMO2	ICO	CUBO
1201	0.06	0.07	0.05	0.00	0.00
1211	0.06	0.02	0.04	0.00	0.33
1301	0.01	0.09	0.02	0.00	0.00
1311	0.26	0.26	0.15	0.26	0.11
1321	0.18	0.26	0.31	0.26	0.00
1421	0.07	0.01	0.01	0.00	0.55
1422	0.25	0.18	0.07	0.38	0.00
1431	0.03	0.03	0.14	0.00	0.00
1541	0.04	0.02	0.10	0.00	0.00
1551	0.05	0.05	0.11	0.10	0.00
2101	0.80	0.86	0.79	0.97	0.53
2211	0.77	0.65	0.56	0.64	1.22
2321	0.09	0.07	0.12	0.00	0.00
2331	0.27	0.27	0.50	0.38	0.19
2431	0.03	0.01	0.05	0.00	0.00
2441	0.19	0.18	0.04	0.26	0.22

V. SUMMARY AND CONCLUSIONS

A structural and vibrational analysis of amorphous isomers of the Au_{55} cluster and a comparison with the icosahedron and cuboctahedron structures was presented. Several nearly degenerate amorphous configurations were found to be more stable than the ordered structures. The short range of the n-body interaction potential explains such behavior. The vibrational analysis shows that the cluster normal modes distribution can be used to discriminate between amorphous and ordered structures. A common-neighbor analysis was performed to classify the short-range order of the amorphous clusters. Distorted multilayer icosahedral order characterizes the amorphous structures with the lowest energies. At higher energies but still below the energies corresponding to the ordered structures, the distorted local icosahedral order is the more representative of the amorphous configurations.

In conclusion, the present study gives additional support to the prediction of the existence of amorphous stable structures in metal clusters. The appearing of such structures will depend on the range of the n-body interaction responsible for the metallic cohesion in these systems. Similar results to ours have been found in other metal clusters using different semiempirical potentials and *ab initio* methods. Therefore, the existence of amorphous clusters does not depend on the use of any specific model potential but on the range and screening of the collective interaction between nuclei and electrons. The size dependence of the disorder-order transition in the lowest-energy structures of amorphous metal small particles, as they grow toward the bulk phase, still has to be investigated. Work in such a direction is in progress for gold nanoparticles.[31] The dynamical behavior of the amorphous gold particles and its connection with recent HRTEM experiments[7] will also be the subject of future investigations.

ACKNOWLEDGMENTS

This work was supported by the Supercomputer Center DGSCA-UNAM, DGAPA-UNAM Project No. IN108296, and CONACYT-México under Project No. 4021-E. A.P.A. acknowledges financial support from CONACYT-Mexico.

[1] J.P. Rose and R.S. Berry, J. Chem. Phys. **98**, 3262 (1993).
[2] S. Tehuacanero, R. Herrera, M. Avalos, and M.J. Yacamán, Acta Metall. Mater. **40**, 1663 (1992).
[3] F.H. Stillinger and T.A. Weber, Phys. Rev. A **25**, 978 (1982).
[4] F.H. Stillinger and T.A. Weber, Phys. Rev. A **28**, 2408 (1983).
[5] J.Y. Yi, D.J. Oh, and J. Bernholc, Phys. Rev. Lett. **67**, 1594 (1991).
[6] A. Sachdev, R.I. Masel, and J.B. Adams, Z. Phys. D **26**, 310 (1993).
[7] W. Krakow, M.J. Yacamán, and J.L. Aragón, Phys. Rev. B **49**, 10 591 (1994).
[8] I.L. Garzón and J. Jellinek, Z. Phys. D **20**, 235 (1991).
[9] S. Sawada and S. Sugano, Z. Phys. D **24**, 377 (1992).
[10] G. D'Agostino, A. Pinto, and S. Mobilio, Phys. Rev. B **48**, 14 447

(1993).
[10] X. Yu and P.M. Duxbury, Phys. Rev. B **52**, 2102 (1995).
[11] M.A. Marcus, M.P. Andrews, J. Zegenhagen, A.S. Bommannavar, and P. Montano, Phys. Rev. B **42**, 3312 (1990).
[12] A. Pinto, A.R. Pennisi, G. Faraci, G. D'Agostino, S. Mobilio, and F. Boscherini, Phys. Rev. B **51**, 5315 (1995).
[13] D. Faken and H. Jónsson, Comput. Mater. Sci. **2**, 279 (1994), and references therein.
[14] A. Posada-Amarillas and I.L. Garzón, Phys. Rev. B **53**, 8363 (1996).
[15] R.P. Gupta, Phys. Rev. B **23**, 6265 (1981).
[16] F. Ducastelle, J. Phys. (Paris) **31**, 1055 (1970).
[17] V. Rosato, M. Guillope, and B. Legrand, Philos. Mag. A **59**, 321 (1989).
[18] J. Jellinek, in *Metal-Ligand Interactions*, edited by N. Russo and D. R. Salahub (Kluwer Academic, Dordrecht, 1996), p. 325.
[19] F. Cleri and V. Rosato, Phys. Rev. B **48**, 22 (1993).
[20] J. Jellinek and I.L. Garzón, Z. Phys. D **20**, 239 (1991).
[22] I.L. Garzón and J. Jellinek, in *Physics and Chemistry of Finite Systems: From Clusters to Crystals*, edited by P. Jena, S.N. Khanna, and B.K. Rao (Kluwer Academic, Dordrecht, 1992), Vol. I, p. 405.
[23] I.L. Garzón and J. Jellinek, Z. Phys. D **26**, 316 (1993).
[24] M.J. López and J. Jellinek, Phys. Rev. A **50**, 1445 (1994).
[25] S. Carnalla, A. Posada, and I.L. Garzón, Nanostruct. Mater. **3**, 385 (1993).
[26] A. Posada-Amarillas and I.L. Garzón, Phys. Rev. B (to be published).
[27] L. Verlet, Phys. Rev. **159**, 98 (1967).
[28] See Refs. 8 and 21 for a description on how to simulate liquidlike clusters.
[29] J.D. Honeycutt and H.C. Andersen, J. Phys. Chem. **91**, 4950 (1987).
[30] J.P.K. Doye, D.J. Wales, and R.S. Berry, J. Chem. Phys. **103**, 4234 (1995).
[31] A. Posada-Amarillas and I.L. Garzón (unpublished).